



**Assessment of Using the Surface Source Approach
in 3-D Neutronics of Fusion Systems**

T.D. Bohm, B. Smith, M.E. Sawan, P.P.H. Wilson

August 2009

UWFDM-1368

***FUSION TECHNOLOGY INSTITUTE
UNIVERSITY OF WISCONSIN
MADISON WISCONSIN***

**Assessment of Using the Surface Source
Approach in 3-D Neutronics of Fusion Systems**

T.D. Bohm, B. Smith, M.E. Sawan, P.P.H. Wilson

Fusion Technology Institute
University of Wisconsin
1500 Engineering Drive
Madison, WI 53706

<http://fti.neep.wisc.edu>

August 2009

UWFDM-1368

Abstract

The accuracy of the results obtained using the surface source write/read feature of MCNP for toroidal fusion systems was assessed. Techniques that enhance the effectiveness of the surface source method were identified. Accurate results can be obtained for a specific component in a fusion system by either inserting the detailed component CAD geometry in the full model for the fusion system or utilizing the surface source approach provided that the surface source and associated reflective boundaries are extended beyond the component of interest by at least ~10 cm and the surface source is placed as close as possible to the front surface of that component.

1. Introduction

The surface source write/read capability in the 3-D neutronics Monte Carlo code MCNP [1] is critical to efficient neutronics modeling of components in fusion systems, allowing a problem that involves a single component to be modeled on a small domain without losing the correct neutron source distribution in phase space. This feature has been implemented in the Direct Accelerated Geometry MCNP (DAG-MCNP) code [2] developed at the University of Wisconsin. In this code, the neutronics calculations are performed directly in the CAD solid model that allows preserving the geometrical details without any simplification and eliminates possible human error in modeling the geometry for MCNP. The surface source capability is of particular interest when applied to the geometrically complex fusion systems where detailed spatial variations of nuclear parameters are needed in a specific component for which detailed solid models are provided. We applied this capability to ITER where detailed analysis is required for a specific first wall/shield (FWS) module.

The FWS components of ITER protect the vacuum vessel (VV) and magnets from the intense radiation of the fusion reaction [3]. The FWS is segmented into 18 rings of modules in the poloidal direction. Modules are numbered from 1 to 18 progressing poloidally upwards from the bottom of the inboard side to the bottom of the outboard side. Detailed nuclear analysis was performed previously for a design configuration of the FWS Module 13 [4]. High-resolution nuclear heating results were created for use in computational fluid dynamics simulations. In that analysis a hybrid 1-D/3-D model was used in which the detailed CAD model of Module 13 was inserted into a 1-D cylindrical model, creating a 1-D/3-D cylindrical hybrid model with a uniformly distributed isotropic 14.1 MeV neutron source in the plasma zone between the inboard and outboard first walls. The neutron wall loading was normalized to the value obtained from 3-D calculations for the full ITER plasma chamber with the exact source distribution [5]. The source in the hybrid 1-D/3-D approach does not accurately represent the angular and energy distribution of neutrons incident on the front surface of Module 13, and could lead to erroneous results. To determine the importance of correctly modeling the neutron source, we performed calculations for a FWS Module 13 configuration utilizing the surface source capability and compared the results to calculations performed with the hybrid 1-D/3-D approach [6]. A surface source was written using the 3-D model of ITER with a detailed plasma source. The surface source was then used in place of the uniform source at the front surface of the detailed CAD model for Module 13. This properly accounts for contribution from the source and other components in the ITER chamber. Nuclear heating profiles were determined at the FW showing that the hybrid 1-D/3-D approach overestimates nuclear heating as shown in Fig. 1.

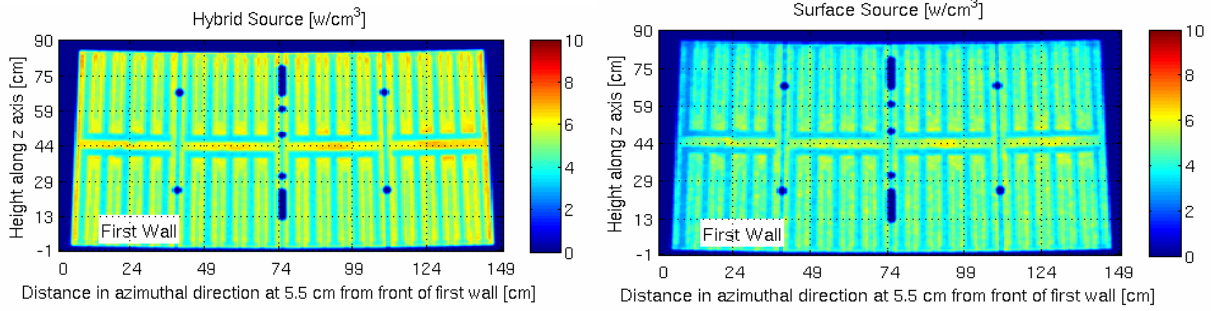


Fig. 1. Nuclear heating in SS zone of ITER FWS Module 13.

While this previous work demonstrated that the surface source methodology gave dramatically different results, they were judged to be more correct only on the basis of engineering judgment that this method reproduced the features of the source more precisely. By also being able to perform neutronics calculations on a detailed solid model placed within a complete 40° sector model of the ITER system, we can now compare the surface source results to a reference result.

In the work reported here, we performed neutronics calculations for a detailed solid model of FWS Module 4 shown in Fig. 2. The calculations were performed with the detailed Module 4 CAD model inserted in the full ITER model. This provides the most accurate nuclear parameters in Module 4 by combining the most complete geometric description with the most complete source description. In addition, we performed calculations for Module 4 using the surface source written at its front surface from calculations with the full ITER model. The results are compared to investigate whether the surface source approach reproduces the accurate results from the full model calculations. To further understand the sensitivity of the results to the size of the surface source and boundary conditions, we performed calculations for a simplified ITER model. In this report, we provide the results of the calculations and make recommendations on how to ensure accurate results utilizing the surface source capability in fusion systems.

2. Results for FWS Module 4 in Full ITER Model

The Module 4 CAD model was inserted in the 40° ITER CAD model, as shown in Figs. 3 and 4, and analysis was performed for the full integrated model using the exact source profile in the plasma. The full ITER model used is a simplified CAD model based on a 40° sector of ITER that includes all ITER components, with detailed structures in each component being suppressed using homogenized material definitions. The model includes dummy port plugs and was previously used in ITER neutronics benchmark calculations [5]. The neutron source was sampled from the exact neutron source profile provided by the ITER International organization and normalized to the fusion power in the ITER 40° sector. The calculations were performed using the DAG-MCNP5 code. This simulation used a total of 500 million source particles over 240 cpu-days on thirty 2.66 GHz Intel Core2 processors. A high-resolution mesh tally with elements <1 cm on the side was superimposed over the CAD geometry of Module 4 yielding 1-sigma statistical errors $<15\%$ locally.

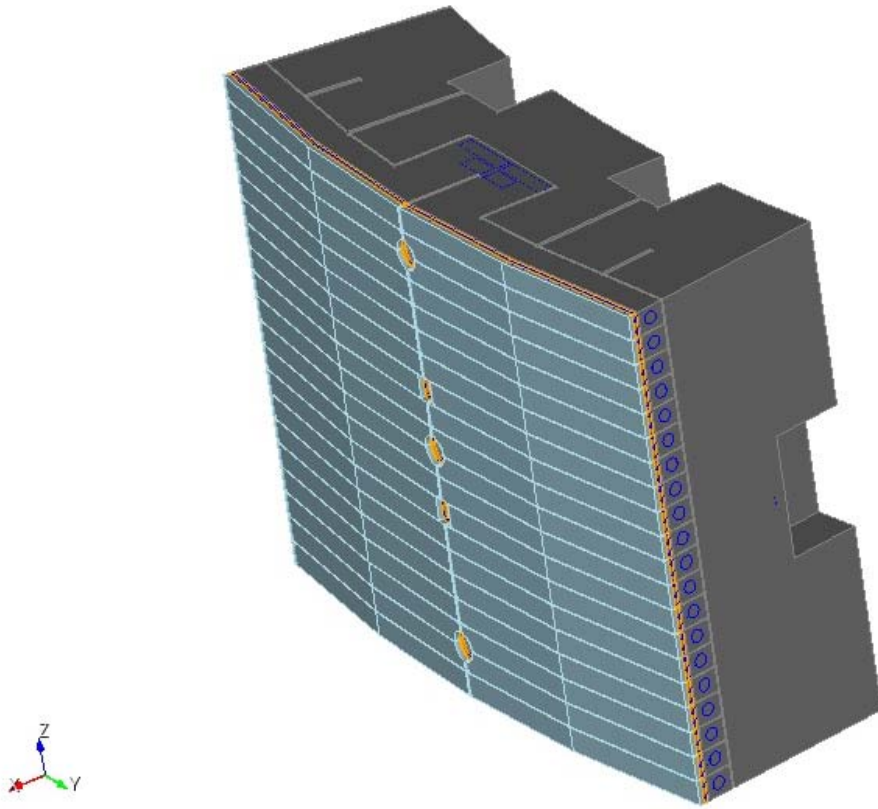


Fig. 2. Module 4 CAD model.

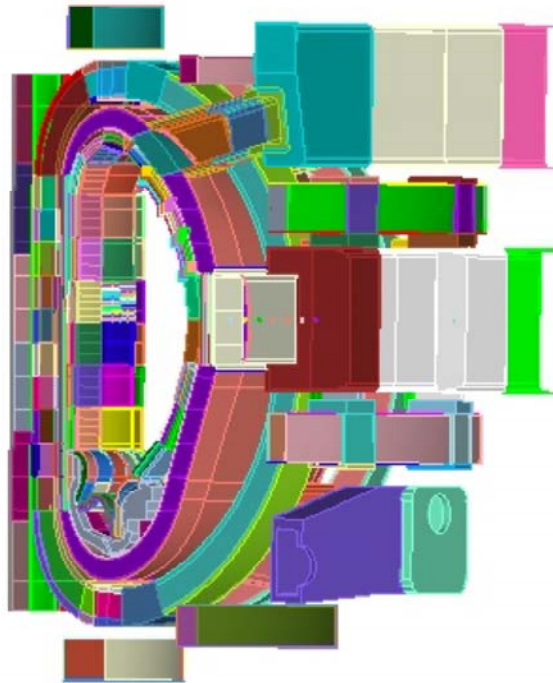


Fig. 3. The Module 4 CAD model inserted into the 40° ITER CAD model.

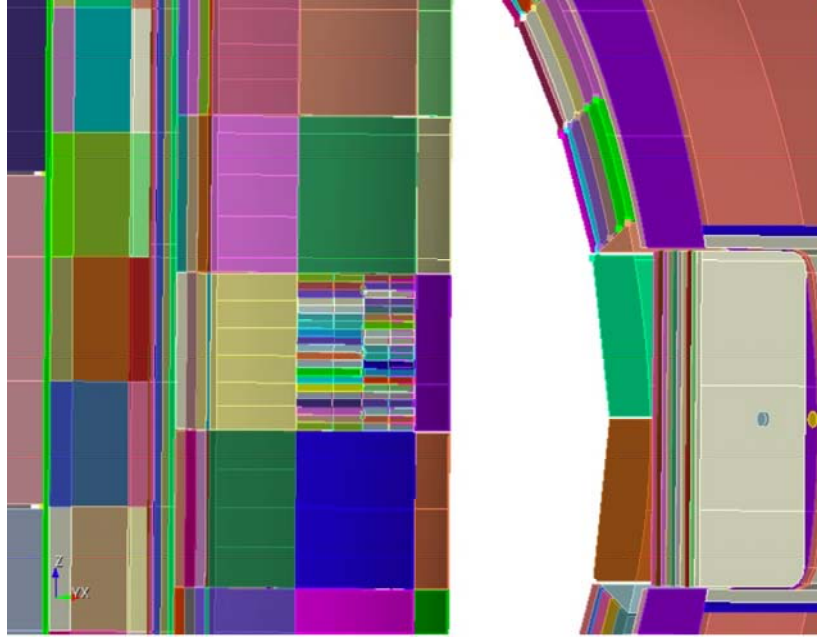
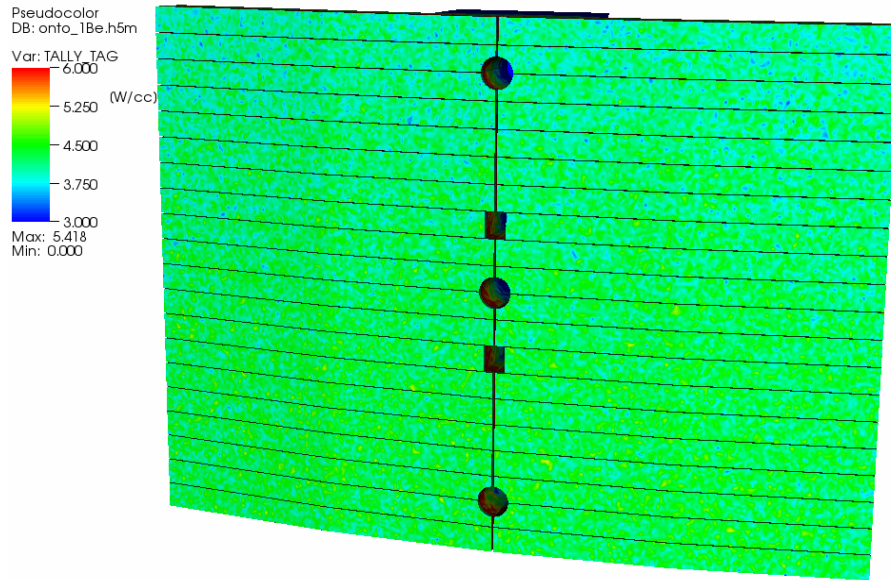


Fig. 4. Module 4 in the full model (zoomed in).

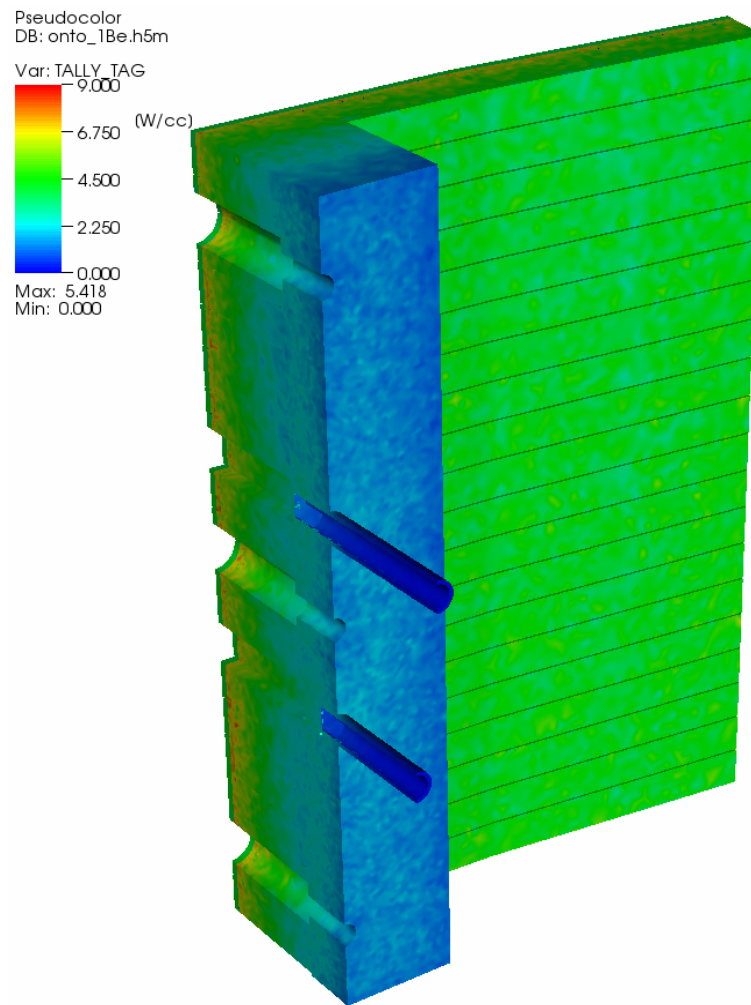
Figure 5 shows the nuclear heating distribution in the FW. The vertical gradient in nuclear heating is a result of the vertical gradient of neutron wall loading at Module 4 with higher values at the lower edge that faces the center of the plasma with peak source density. Higher heating in the CuCrZr heat sink behind the Be plasma facing layer is clearly shown. Figure 6 shows nuclear heating in the CuCrZr and Fig. 7 gives nuclear heating in the steel used in the FW.

3. Results for FWS Module 4 Using Surface Source

Placing the entire FWS Module 4 CAD geometry in the 3-D 40° ITER model significantly extended the simulation time required to yield low statistical error for high-fidelity mesh tallies. Instead, using the recently implemented surface source feature, Module 4 can be analyzed in a radial approximation using the detailed source of the 3D ITER model. A surface source was written using the 3-D 40° ITER model that has a detailed neutron source distribution provided by the ITER IO. A surface was placed directly in front of the Module 4 FW as shown in Fig. 8. The location, angle, and energy of all particles crossing the surface were recorded to a file. Using the 3-D ITER source profile, 450 million source particles were simulated (approximately 41 cpu-days) resulting in 29.3 M surface crossings. The results were normalized to the fusion power in the ITER 40° sector. The energy spectra of neutrons and gamma photons crossing the surface into Module 4 are given in Figs. 9 and 10. The angular distributions are given in Fig. 11. Only 44% of the neutrons incident on Module 4 are uncollided source neutrons at 14 MeV due to significant secondary neutrons from the chamber components. The average neutron energy is 6.66 MeV. The number of secondary gamma photons incident on Module 4 is 46% of the number of neutrons. The average gamma energy is 1.45 MeV. The neutrons have a slightly more perpendicular angular distribution compared to the secondary gammas due to the direct contribution from source neutrons at the center of the plasma.



(a) Front View



(b) Back View

Fig. 5. Nuclear heating in FW of Module 4.

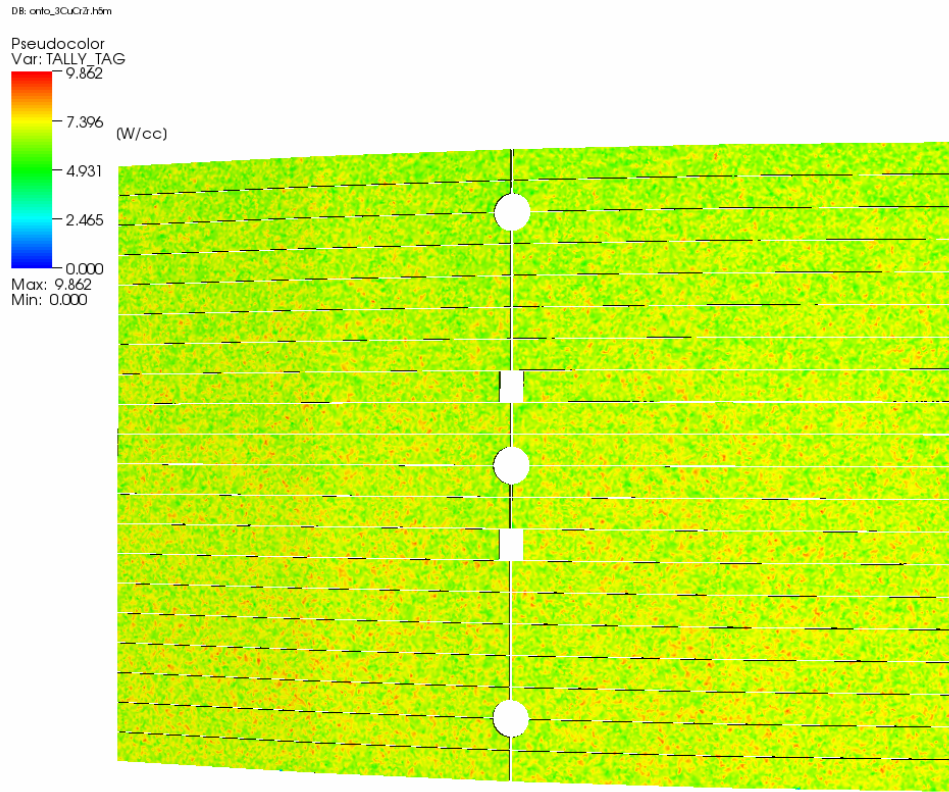


Fig. 6. Nuclear heating in CuCrZr.

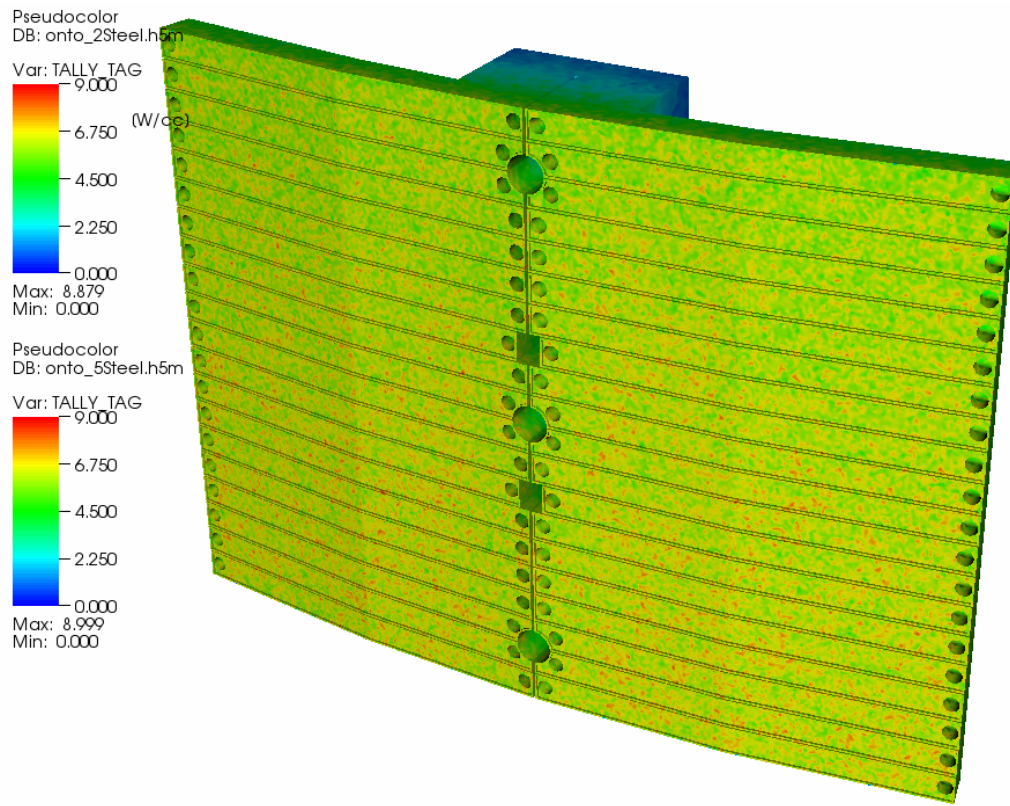


Fig. 7. Nuclear heating in the steel of the FW.

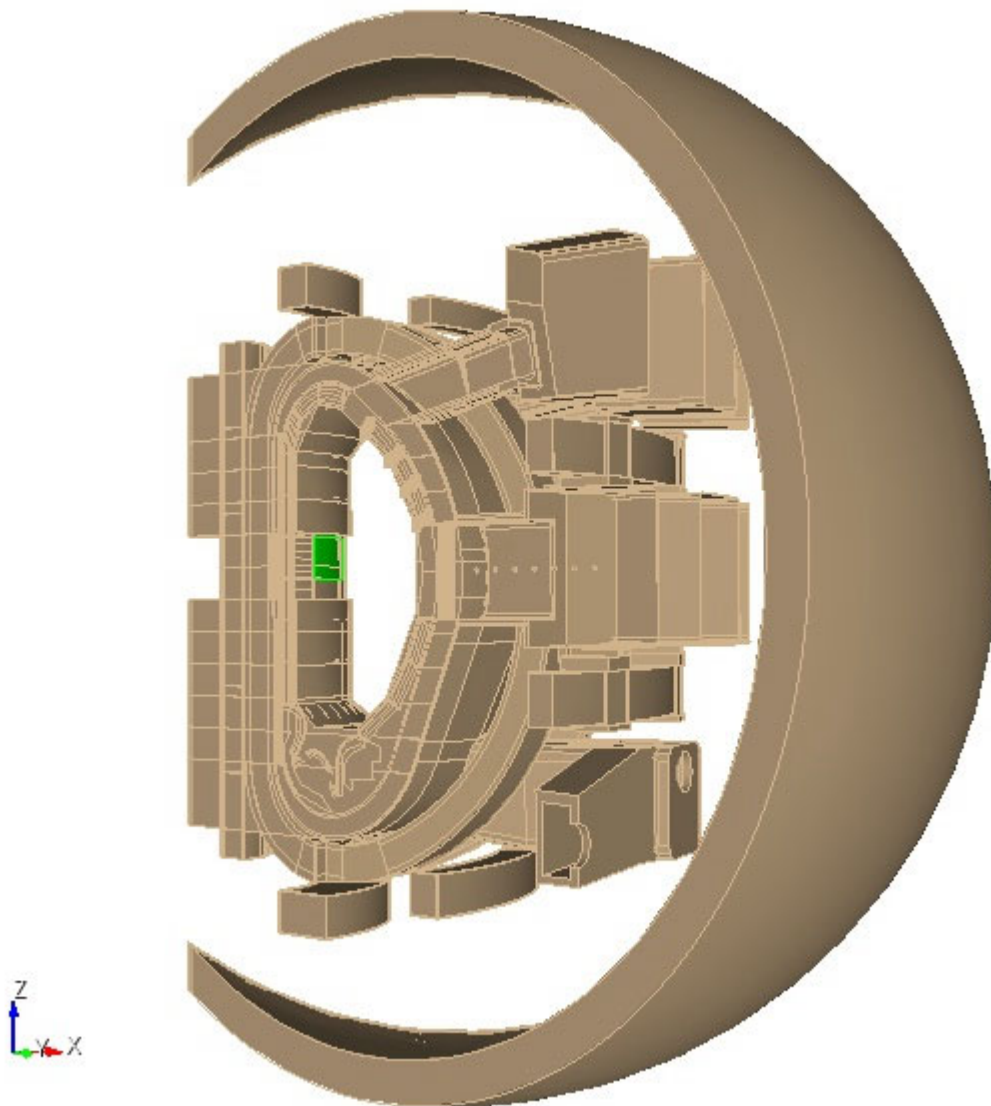


Fig. 8. Surface source (green) for Module 4 inserted into the 40° ITER model.

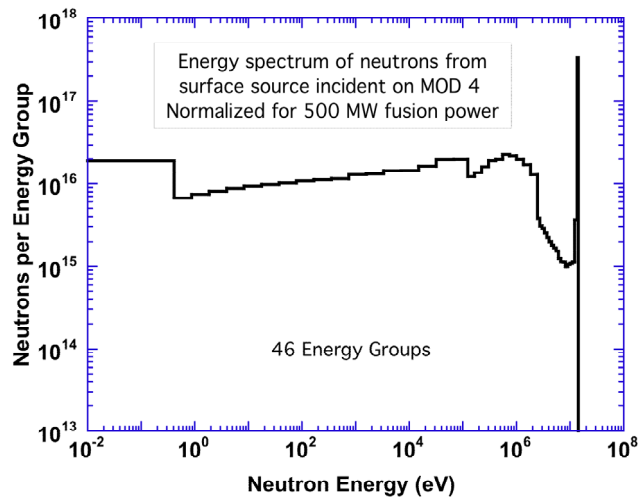


Fig. 9. Energy spectrum of neutrons incident on Module 4.

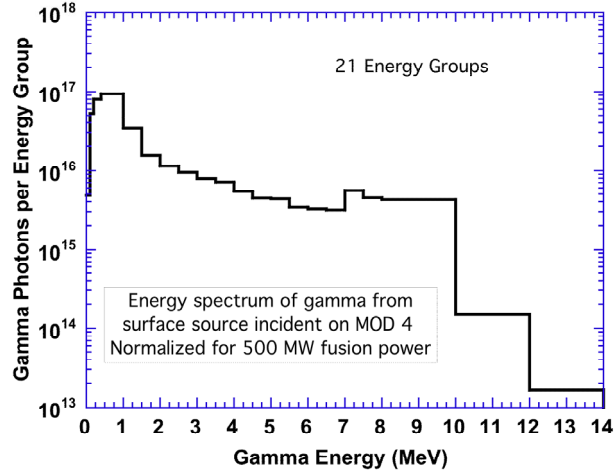


Fig. 10. Energy spectrum of gamma photons incident on Module 4.

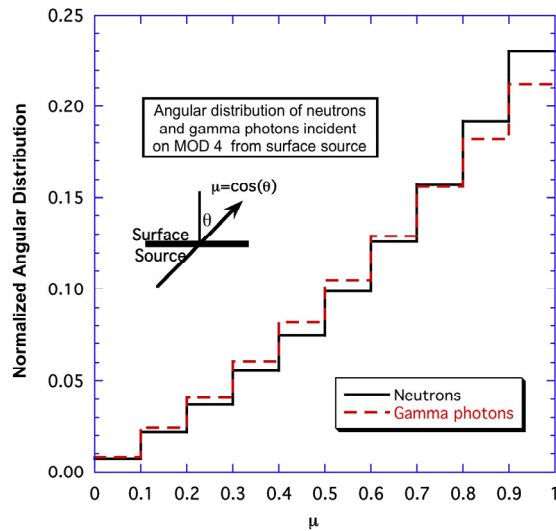


Fig. 11. Angular distribution of neutrons and photons incident on Module 4.

A Module 4 surface source model was created with a surface added directly in front of the FW, as shown in Fig. 12, that corresponds to the surface from the 3-D 40° ITER model on which the surface source was recorded. This surface covers Module 4 and half of the surrounding gap. The surface source is slightly offset (1 cm) from the front surface of Be. While the effect of reflection into the chamber from surrounding components is accounted for by the surface source, contribution at the sides of the module will depend on the boundary conditions used. The CAD geometry was surrounded by reflecting boundaries through the surrounding gaps in the poloidal and toroidal directions to simulate the effect of neighboring FWS modules. Volumes from the 40° ITER model were inserted behind the Module 4 CAD model to achieve proper reflection. Source particles were then “born” on the surface corresponding to the surface source. Each recorded particle crossing from the 40° ITER model was read as a source particle in the Module 4 surface source model. No additional normalization is needed since the initial normalization used when writing the surface source is carried over.

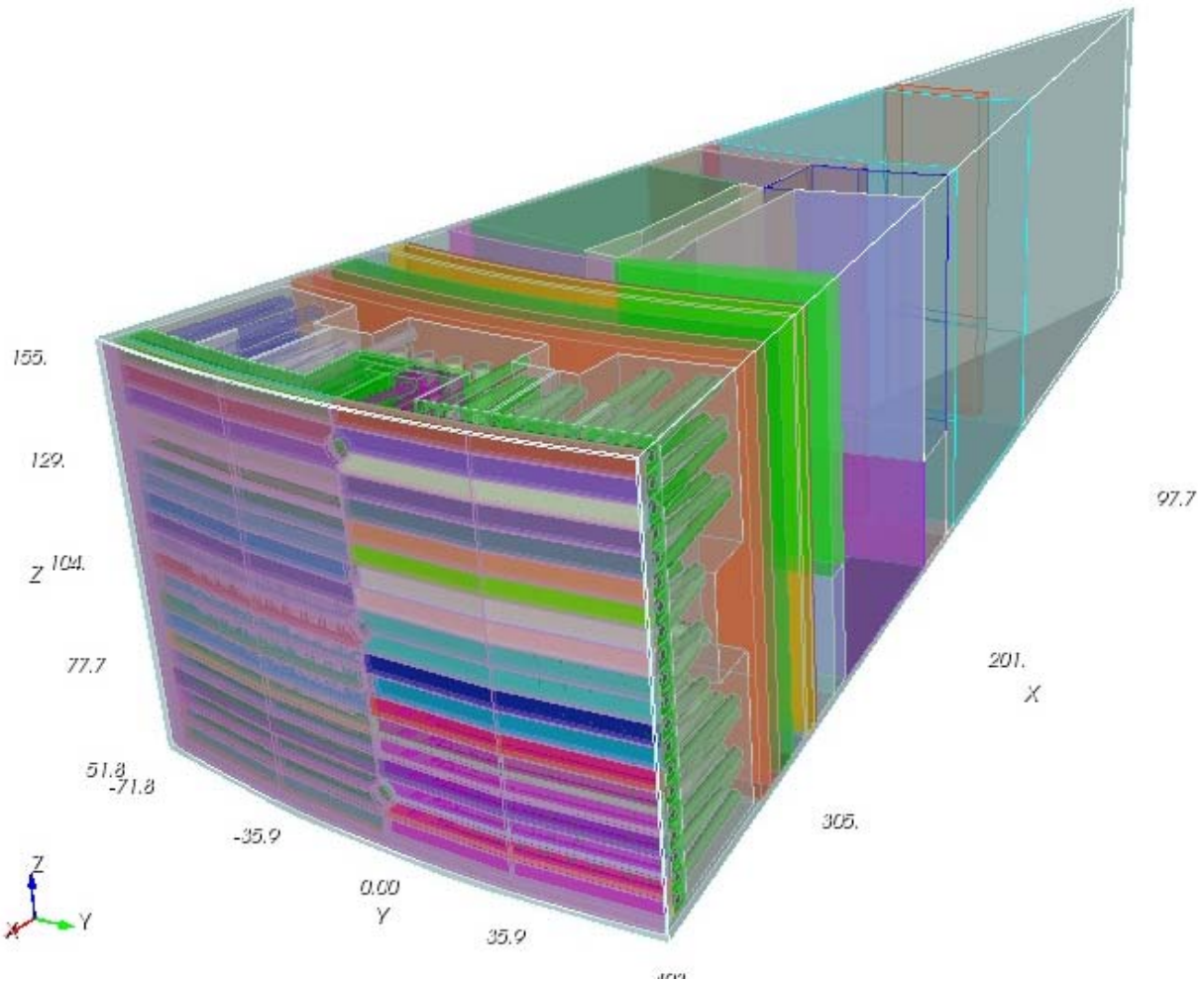


Fig. 12. Module 4 CAD model used with surface source.

Simulations were performed repeating each surface crossing 10 times, with different random numbers each time (about 37 cpu-days). Particles originate from the surface source, preserving angle, energy, weight, and position calculated in the 40° ITER model. Hence, the mesh analysis simulates 293 M particles entering Module 4, the same number as would enter if 4.5 B particles (which would have required approximately 2200 cpu-days) were modeled in the entire ITER plasma region. Both the plasma volume and outboard FWS are absent from the Module 4 surface source model. Instead, all secondary contribution from the inboard and outboard FWS modules in the plasma chamber is accounted for in the surface source. A mesh with 5 mm edge-length was used and energy deposition mesh tallies were generated with 1-sigma statistical error <15% locally. Figs. 13 and 14 show nuclear heating distribution at several sections of the first wall.

4. Comparison between Results with Full Model and Surface Source

Using the surface source resulted in considerable improvement in comparison to the uniform source of the 1-D/3-D hybrid geometry analysis. Nuclear heating results for Module 13 with the surface source approach were compared previously to the results of the hybrid 1-D/3-D approach and indicated that the approximations in the hybrid 1-D/3-D approach yield up to ~30%

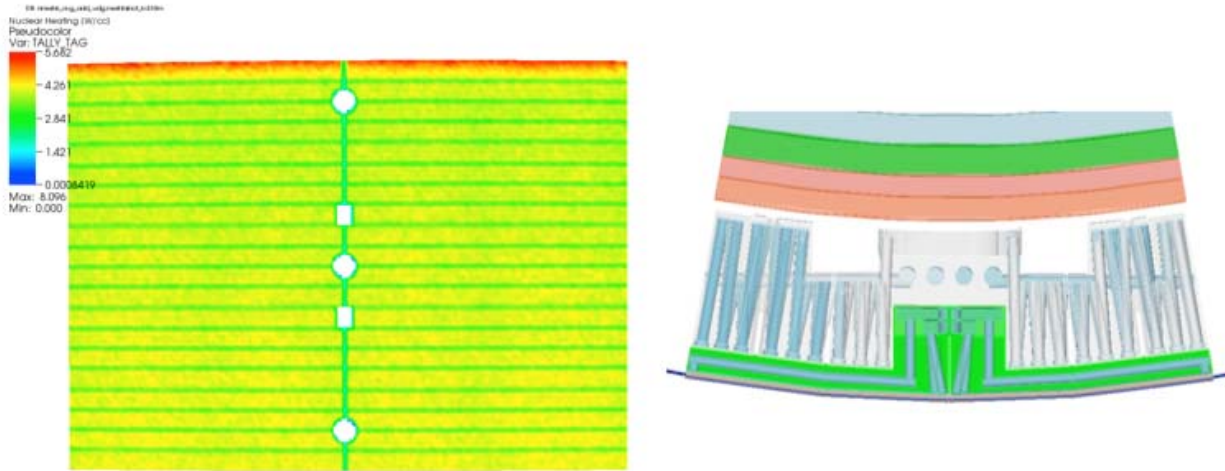


Fig. 13. Cylindrical cut at $r=403.3$ cm through beryllium.

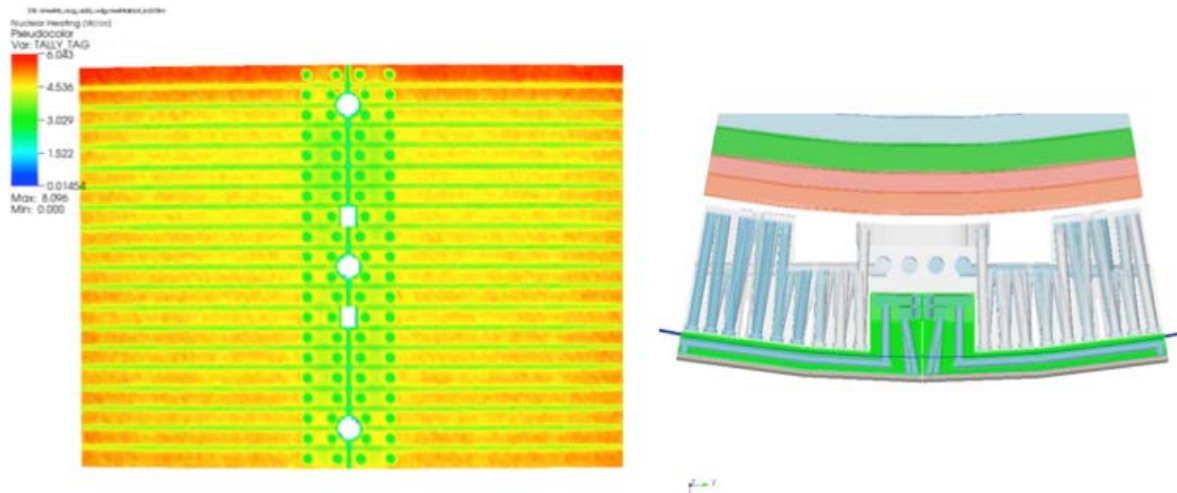


Fig. 14. Cylindrical cut at $r=396.8$ cm through the back of the steel first wall.

overestimate in nuclear heating [6]. Results from the Module 4 mesh analysis with surface source, shown in Figs. 13 and 14, suggest that the surface source approach might introduce artifacts as indicated by the high nuclear heating observed at the top of the module compared to the results in Figs. 5-7 obtained using the full ITER model.

Table 1 compares the total number of neutrons crossing the front surface into module 4. Neutron crossing is slightly ($<1\%$) higher with surface source due to the slight offset of surface source from the front surface of the module combined with the reflecting boundary use (see Section 6, below). The front surface of Module 4 was divided vertically into 20 horizontal segments and number of neutrons crossing the top and bottom segments into the module was compared for different angle bins in the two calculations. Examining the results in Table 2 indicates that neutrons crossing at the bottom of the module, which faces the center of the plasma with peak source density, are more perpendicular to the front surface than at the top. Using the surface source overestimates neutrons crossing into the module at the top with the most

Table 1. Particles crossing into whole module per second.

Uncollided neutrons	Full model	3.34×10^{17}
	Surface source	3.37×10^{17}
	% change	0.9%
Total neutrons	Full model	7.66×10^{17}
	Surface source	7.68×10^{17}
	% change	0.3%

Table 2. Angular distribution of neutrons crossing into module per second at top and bottom.

		Top	Bottom
$\mu=0.9-1.0$ (perpendicular)	Full model	7.78×10^{15}	9.39×10^{15}
	Surface source	8.02×10^{15}	9.46×10^{15}
	% change	3.1%	0.8%
$\mu=0.0-0.1$ (tangential)	Full model	2.66×10^{14}	2.70×10^{14}
	Surface source	3.27×10^{14}	2.75×10^{14}
	% change	22.8%	1.9%
Total	Full model	3.71×10^{16}	3.95×10^{16}
	Surface source	3.94×10^{16}	3.95×10^{16}
	% change	6.2%	0%

pronounced overestimate in the tangential component. This is due to reflection by the top reflecting boundary of the neutrons coming from the surface source (that is offset from the front surface of module) in a tangential direction at the top. This contributes to the higher heating values observed at the top of the module compared to the bottom when the surface source is used.

Table 3 compares total nuclear heating calculated in each material of the FWS module. It is clear that using the surface source approach leads to some modest overestimation of nuclear heating. This small increase in total heating is due to a substantial overestimate of nuclear heating near the top of the module that follows from the overestimate in the neutron current. In combination, an accurate surface source and a reflecting boundary effectively mirrors the source across that boundary. In the case of the ITER model there is a local maximum in the source density near the bottom of Module 4 (system midplane) that gets effectively reflected to the top of the adjacent module (Module 5). Reflection at the top surface represents particles that come from such a “shadow” source. In other words, it assumes higher wall loading than should be at these adjacent modules at the top.

Table 3. Overestimate in nuclear heating (MW) resulting from surface source.

	Full ITER Model	Surface Source Model	% Overestimate
Beryllium	0.0535	0.0543	1.50%
CuCrZr	0.0350	0.0356	1.71%
Steel	0.757	0.790	4.36%
Water	0.150	0.157	4.67%

5. Assessment of Accuracy of Surface Source Approach

In order to investigate the artifact indicated by the peak in nuclear heating observed at the top of the module and the overestimate in total nuclear heating obtained with the surface source, we performed analysis with the native geometry version of the MCNPX code on simplified 3-D cylindrical models of the ITER machine and Module 4. For this analysis, a simplified baseline model was created which is a 3-D 40° model with homogenized materials. This model includes reflective boundaries at toroidal angles of -20° and +20° and is centered azimuthally about Module 4 which spans from -10° to +10°. The model is 800 cm high and has a uniform source in the volume $z=0-100$ cm and $r=519-719$ cm. Note that Module 4's axial extent is from $z=50-150$ cm, just above the midplane and subject to similar angular distribution of uncollided neutrons as the Module 4 in the real ITER model. The results of this analysis are expected to be qualitatively the same as the true Module 4, although quantitatively different due to the approximations made here. Figures 15 and 16 show the 3-D simplified baseline model. This model is used to generate a surface source for analysis using the surface source method and to serve as the "exact" model for comparison purposes.

The surface source model is truncated azimuthally with reflective boundaries at Module 4 (-10° to +10°) and is truncated axially at the same location as the surface source. The outboard importance is set to 0 in this model and the surface source offset is 1 cm from the front of the Module 4 first wall (toward the plasma). Figure 17 shows the surface source model geometry. For this work, three surface source cases are examined:

1. The surface source is the same size as module 4 ($z=50-150$ cm)
2. The surface source is extended 10 cm above and below module 4 ($z=40-160$ cm)
3. The surface source is extended 25 cm above and below module 4 ($z=25-175$ cm)

Figure 18 shows the FW heating ratio as a function of height along Module 4 for case 1 (extension=0 cm). The heating ratios are found by dividing the results from the surface source case by the results from the baseline case and are shown at 8 different depths in the FW. Figure 18 clearly shows the peak in heating near the top of Module 4 as seen in the earlier CAD based calculations. Note that the FW heating determined using the surface source case 1 is quite close to the baseline until reaching the top 10-15 cm. The average uncertainty (at the 1 σ level) in the heating tallies used for Fig. 18 is 1.5% giving 2.1% uncertainty in the heating ratios. Figures 19-21 have similar uncertainties.

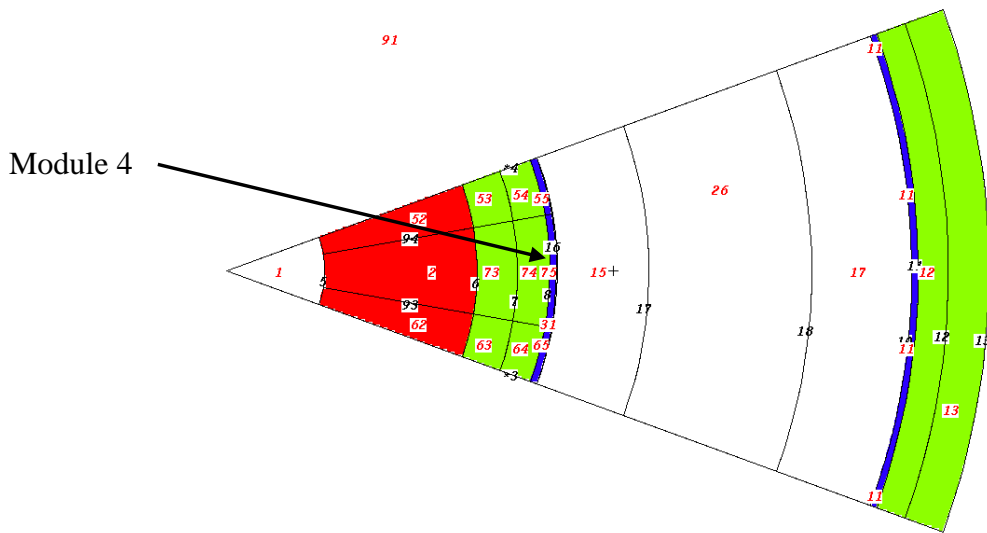


Fig. 15. Horizontal slice through simplified baseline model.

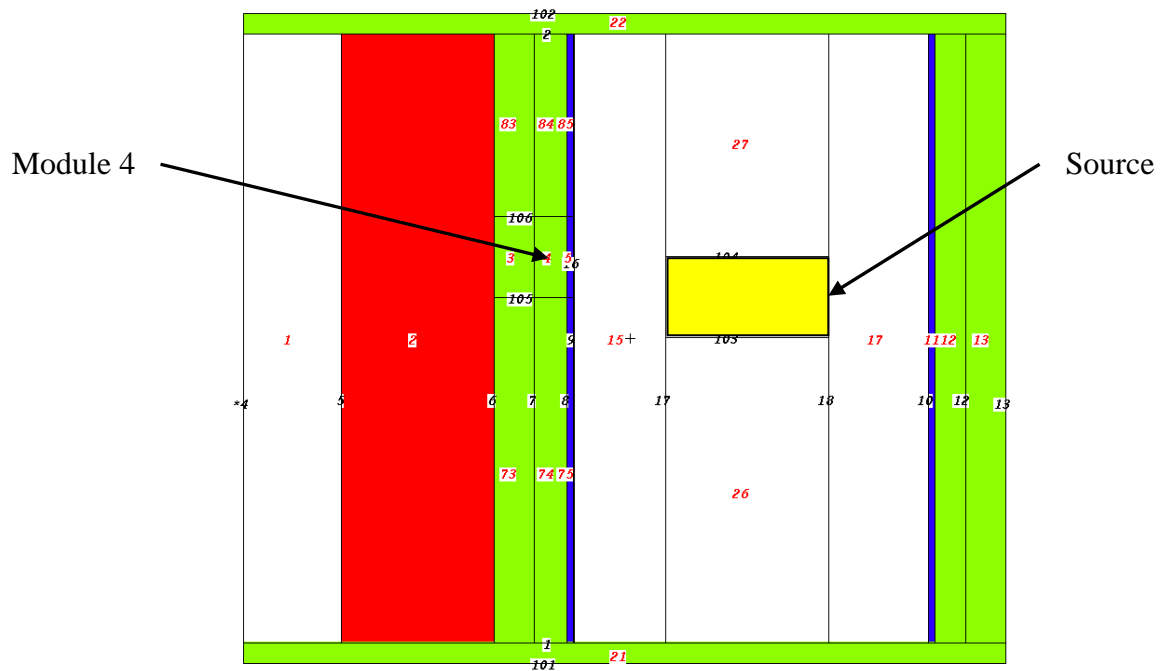
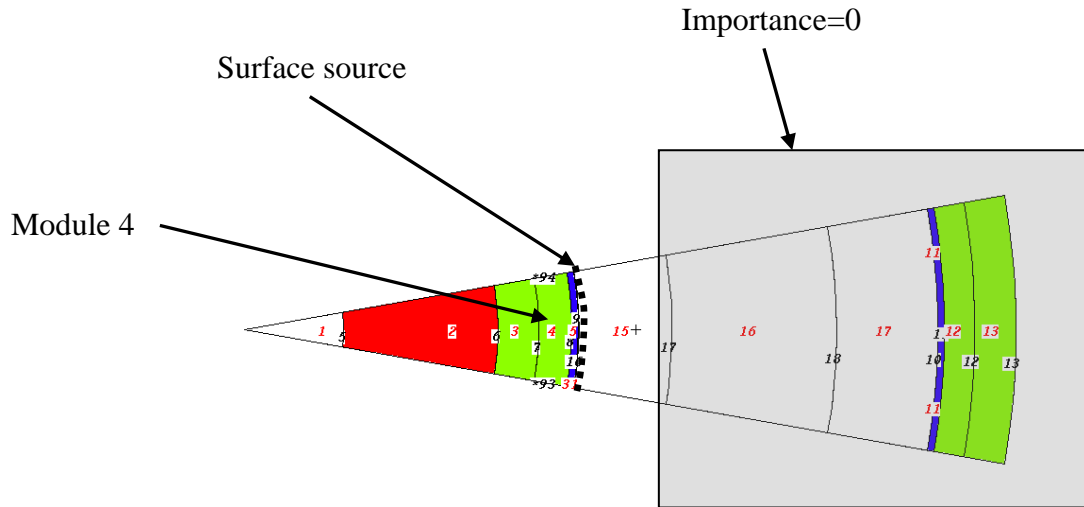


Fig. 16. Vertical slice through simplified baseline model.



91

Fig. 17. Horizontal slice through surface source model.

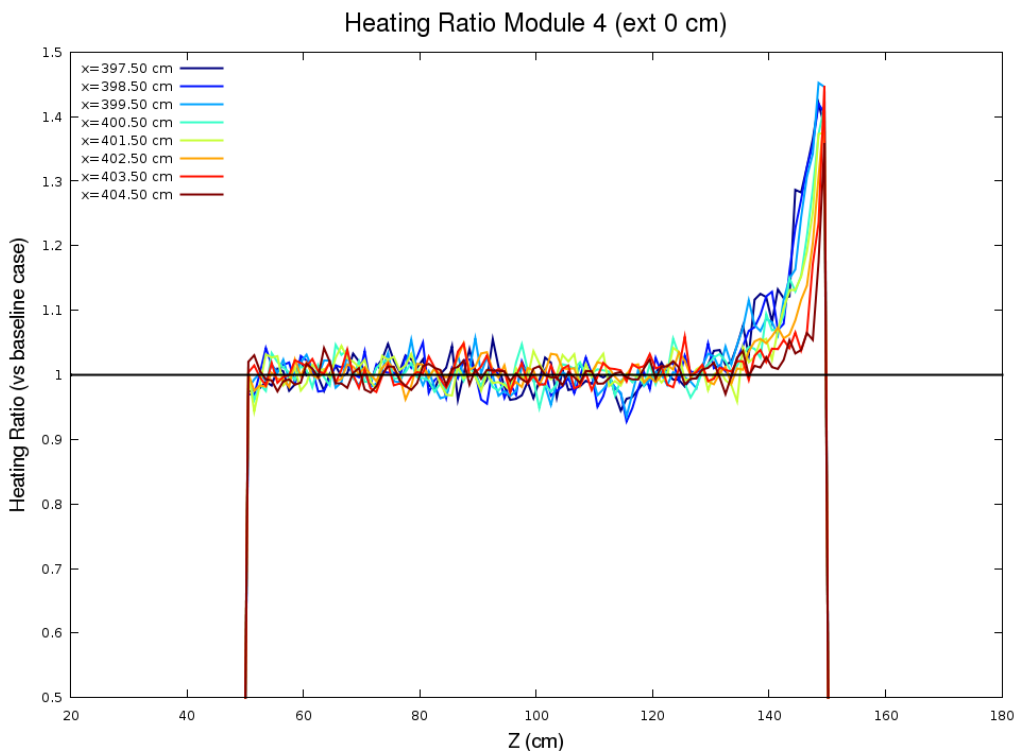


Fig. 18. FW heating ratio as a function of height along Module 4 for case 1 (extension=0 cm).

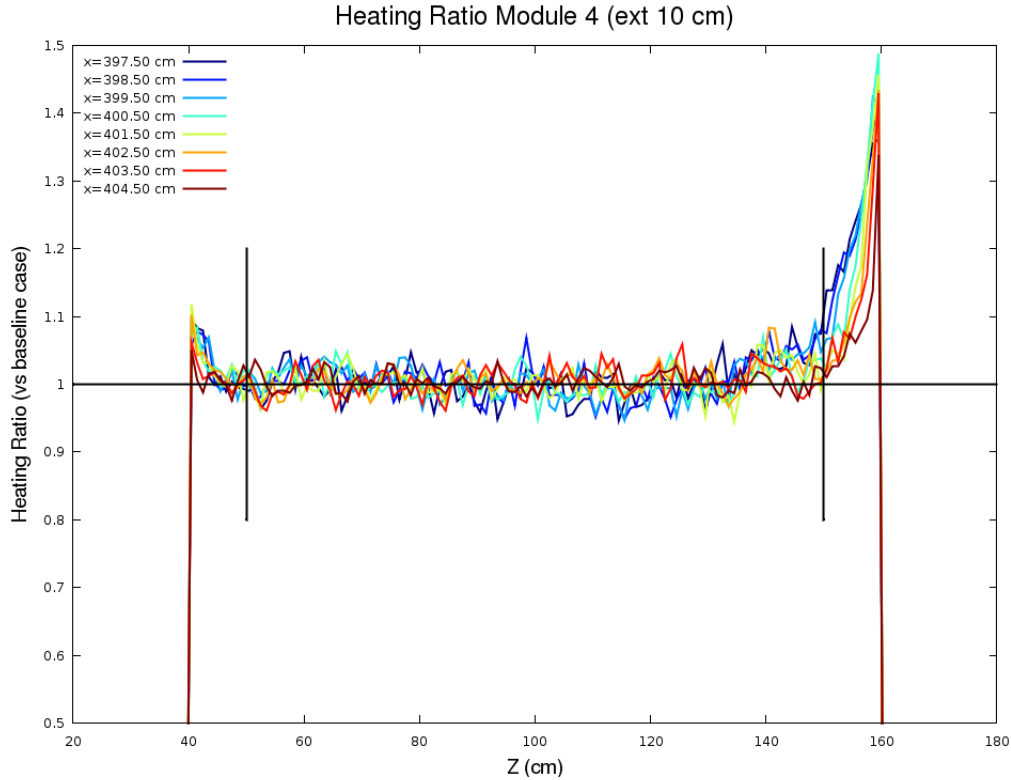


Fig. 19. FW heating ratio as a function of height along Module 4 for case 2 (extension=10 cm).

Figure 19 shows the FW heating ratio as a function of height along Module 4 for case 2 (extension=10 cm). Vertical lines on the figure indicate the top and bottom boundaries of Module 4. Figure 19 shows a peak in heating at the top and bottom of the surface source model near the reflective boundaries and beyond Module 4. Note that the FW heating determined using the surface source case 2 is quite close to the baseline at the heights corresponding to Module 4.

Figure 20 shows the FW heating ratio as a function of height along Module 4 for case 3 (extension=25 cm). Vertical lines on the figure indicate the top and bottom boundaries of Module 4. Figure 20 shows peaks in heating that are shifted even further from Module 4 as compared to cases 1 and 2. These peaks correspond to the location of the reflective top and bottom boundaries of the surface source model. Note that the FW heating determined using the surface source case 3 is quite close to the baseline at the heights corresponding to Module 4. The results in Figures 18-20 clearly indicate that the existence and location of the peaks in heating are dependent on the relative location of the reflective boundaries in comparison to the source.

In order to investigate the effect of the surface source offset, the FW heating was determined using a surface source with no offset and no extension beyond Module 4 (case 1). Figure 21 shows the FW heating ratio as a function of height along Module 4 for case 1 (extension=0 cm) with no offset. Note that the peaks in the heating ratio are significantly reduced as compared to the results shown for case 1 with the 1 cm surface source offset (Fig. 18). In particular, note that for the FW heating ratios at the shallow depths, $x=403.4$ cm and $x=404.5$ cm, the peak ratios

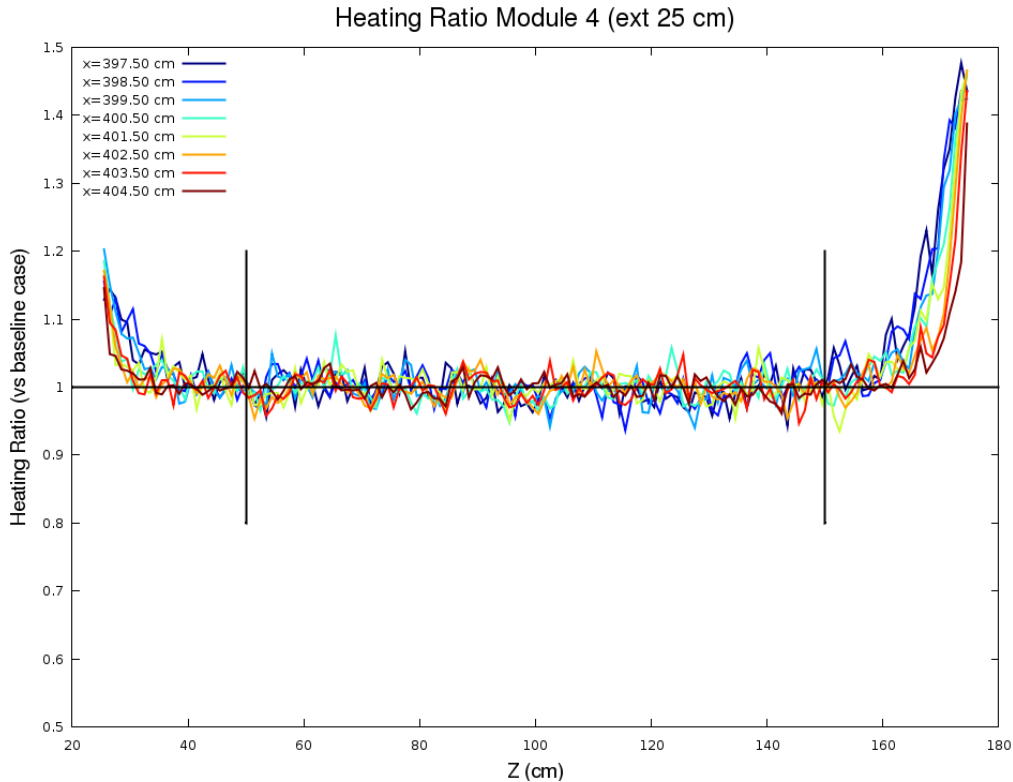


Fig. 20. FW heating ratio as a function of height along Module 4 for case 3 (extension=25 cm).

have gone from 1.45 and 1.36, to 1.33 and 1.18 respectively. These results are highlighted in Fig. 21 with thicker lines.

To better illustrate the differences in Figs. 18-21, Figure 22 shows the FW heating ratio as a function of height along Module 4 at a depth of 0.5 cm ($x=404.5$ cm) for cases 1-3. This figure clearly shows the reduced peaking for case 1 (ext=0 cm) with an offset of 0 cm.

Table 4 compares the total FW heating in Module 4 for the baseline and 3 surface source cases as determined using a combined neutron and photon energy deposition (f6:n,p) tally. Statistical uncertainty for the total heating tallies used in this table is 0.07% (1σ) giving an uncertainty of 0.10% in the heating ratio. Case 1 with the surface source just covering the module overestimates the FW heating by 1.8%. Extending the surface source by 10 cm (case 2) improves the calculation with an overestimate of just 0.4%. Case 3 which has a 25 cm extension shows very close agreement to the baseline case. Finally, for case 1 with no surface source offset, the total FW heating shows an overestimate compared to the baseline case of 1.45%. However, this overestimate is smaller than that seen with a 1 cm surface source offset.

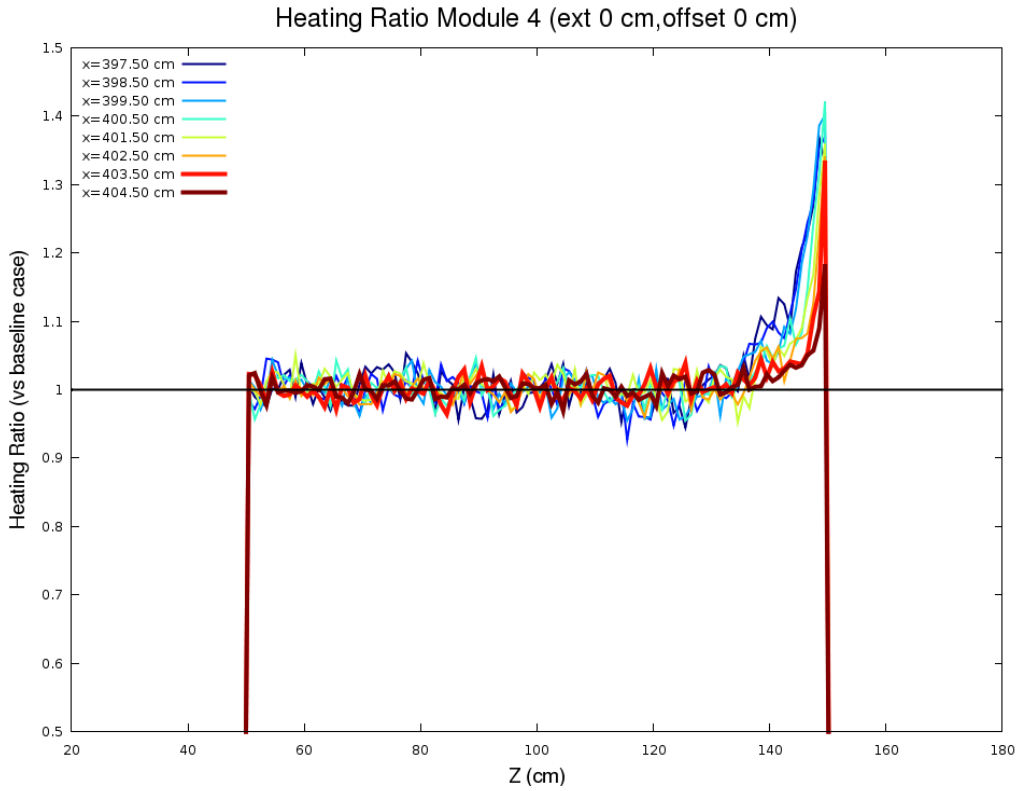


Fig. 21. FW heating ratio as a function of height along Module 4 for case 1 (extension=0 cm) with a surface source offset=0 cm.

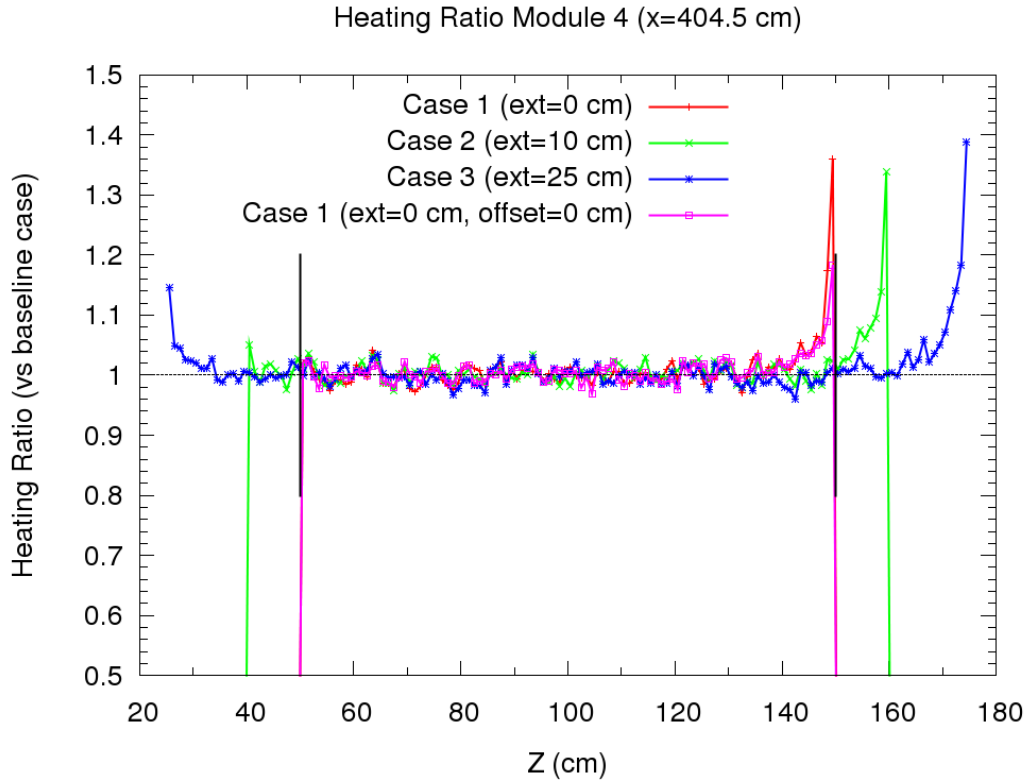


Fig. 22. FW heating ratio as a function of height along Module 4 for cases 1-3 and case 1 with a surface source offset=0 cm.

Table 4. Impact of surface source extent and offset on accuracy of FW nuclear heating.

	Geometry	Source	FW Heating (ratio)
Baseline	full	full	1
Case 1	Mod4, reflective	Mod4 surface source	1.0180
Case 2	Mod4+10 cm, reflective	Mod4+10 cm surface source	1.0038
Case 3	Mod4+25cm, reflective	Mod4+25 cm surface source	0.9992
Case 1 (offset=0 cm)	Mod4, reflective	Mod4 surface source	1.0145

6. Understanding the Sources of Error in the Surface Source Methodology

Figures 23-25 help illustrate the particle tracks that create the overestimation of heating near the top of Module 4 for Case 1. In Figure 23 we see two particle tracks that might normally deposit energy into Module 5. Note that since more of the source volume is near the bottom of Module 4, there will be fewer particle tracks entering Module 5 than Module 4, and, the particle tracks near the interface between Modules 4 and 5 will have a more tangential angular distribution. In Fig. 24 we see that with the reflective boundary, these same two tracks are *always* redirected back into Module 4, even though there is no corresponding source volume in line with Module 5 which would create more track uniformity at the Module 4/Module 5 interface. Finally, in Fig. 25 we see that since we are using a volumetric tally for heating, even if the surface source is at the front surface of Module 4, there is still some particle reflection near the top of the module. However, the peaking is reduced particularly at shallow depths due to elimination of contribution from tracks reflected in the offset region.

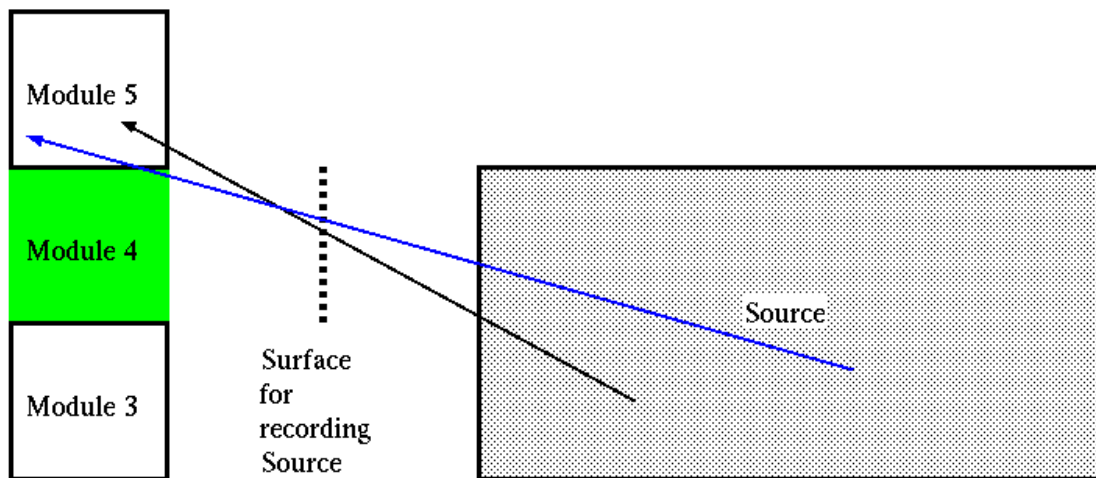


Fig. 23. Baseline case showing two particle tracks entering Module 5.

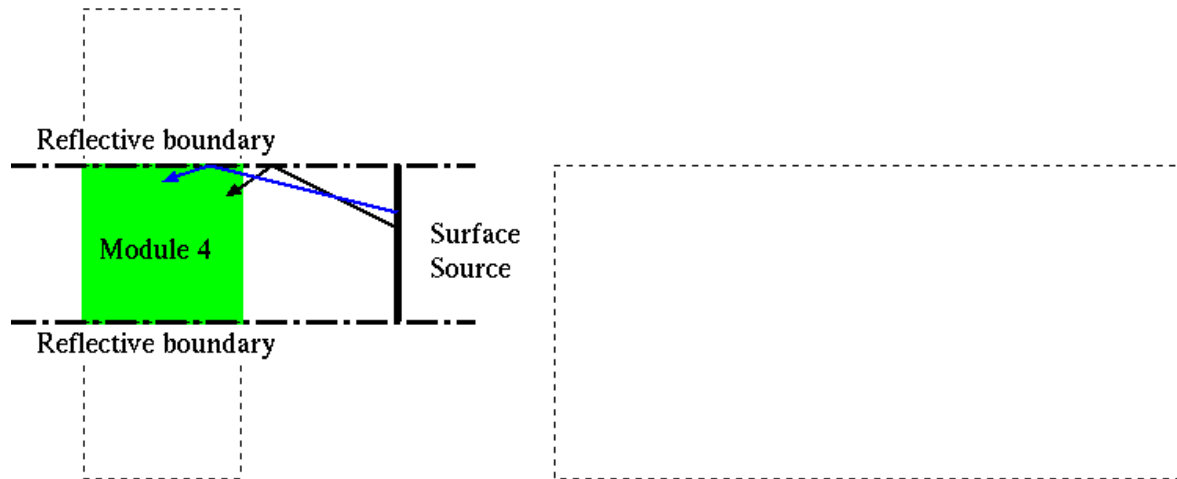


Fig. 24. Case 1 showing how the reflective boundary forces particle tracks to enter Module 4.

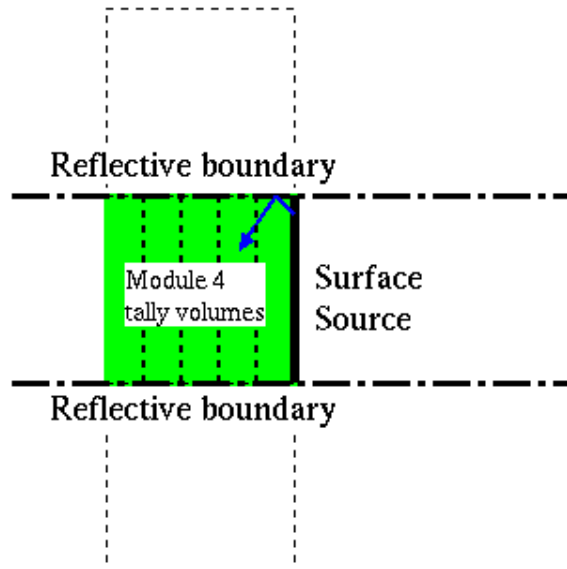


Fig. 25. Case 1 showing a surface source with no offset and illustrating how a volumetric tally will see some of the peaking effect as seen with an offset surface source.

7. Conclusions

The results of the analysis performed for ITER FWS Module 4 indicate that using the surface source approach can produce accurate results that are in agreement with results obtained using the full ITER model with detailed Module 4 CAD model inserted in it. However, the surface source and associated reflecting boundaries should be extended by 10-25 cm beyond the module boundaries to eliminate the local artifacts introduced by the surrounding reflecting boundaries. Additionally, the surface source should be close to the module being analyzed. Based on our analysis, we are confident that accurate results can be obtained by either inserting the module CAD geometry in the full ITER model or utilizing the surface source approach provided that the

surface source and associated reflective boundaries are extended beyond the module of interest by at least ~10 cm.

Using the surface source technique requires more human effort with less computation time. However, using the full model technique (detailed CAD model in 40° ITER CAD model) requires less human effort with more computation time. While the investment of human effort in the surface source technique for a given model may be recovered with repeated use of the same surface source, i.e. analyzing many design iterations of the same FWS module, this benefit has not yet been realized in practice. For the same statistical precision in the results, the total analysis time (human effort plus computation time) may be shorter using the surface source technique.

References

- [1] X-5 Monte Carlo Team, “MCNP-A General Monte Carlo N-Particle Transport Code, Version 5-Volume II: Users Guide,” LA-CP-03-0245, Los Alamos National Laboratory (April 2003, revised 2/1/2008).
- [2] T. Tautges, P.P.H. Wilson, J. Kraftcheck, B. Smith, and D. Henderson, “Acceleration Techniques for Direct Use of CAD-Based Geometries in Monte Carlo Radiation Transport,” Proceedings of International Conference on Mathematics, Computational Methods & Reactor Physics (M&C 2009), Saratoga Springs, New York, May 3-7, 2009.
- [3] ITER Design Description Document, 1.6 Blanket, ITER Document ITER_D_22F3M6 v2.0, ITER IO (2004).
- [4] B. Smith, P. Wilson, and M. Sawan, “Three Dimensional Neutronics Analysis of the ITER First Wall/Shield Module 13,” Proc. IEEE/NPSS 22nd Symposium on Fusion Engineering, Albuquerque, NM, June 17-21, 2007, IEEE (2007).
- [5] P. Wilson, et al., “State of the Art 3-D Radiation Transport Methods for Fusion Energy Systems,” Fusion Engineering and Design, vol. 83, pp. 824-833 (2008).
- [6] B. Smith, P. Wilson, M. Sawan and T. Bohm, “Source Profile Analysis for the ITER First Wall/Shield Modules,” Fusion Science and Technology, August 2009.